SAND--96-2075C
CONF-970324--4

* High G MEMS Integrated Accelerometer

^ Brady R. Davies, Carole Craig Barron, Stephen Montague, James H. Smith, James R. Murray, Todd R. Christenson, Vesta I. Bateman

Integrated Micromechanics, Microsensors, & CMOS Technology Department
Sandia National Laboratories, P.O. Box 5800 MS 1080
Albuquerque, New Mexico 87185-1080

ABSTRACT

This paper describes the design and implementation of a surface micromachined accelerometer for measuring very high levels of acceleration (up to 50,000 G). Both the mechanical and electronic portions of the sensor were integrated on a single substrate using a process developed at Sandia National Laboratories. In this process, the mechanical components of the sensor were first fabricated at the bottom of a trench etched into the wafer substrate. The trench was then filled with oxide and sealed to protect the mechanical components during subsequent microelectronics processing. The wafer surface was then planarized in preparation for CMOS processing using Chemical Mechanical Polishing (CMP). Next, the CMOS electronics were fabricated on areas of the wafer adjacent to the embedded structures. Finally, the mechanical structures were released and the sensor tested.

The mechanical structure of the sensor consisted of two polysilicon plate masses suspended by multiple springs (cantilevered beam structures) over corresponding polysilicon plates fixed to the substrate to form two parallel plate capacitors. The first polysilicon plate mass was suspended using compliant springs (cantilever beams) and acted as a variable capacitor during sensor acceleration. The second polysilicon plate mass was suspended using very stiff springs and acted as a fixed capacitor during acceleration. Acceleration was measured by comparing the capacitance of the variable capacitor (compliant suspension) with the fixed capacitance (stiff suspension).

Keywords: accelerometer, integrated MEMS, micromachined sensors, shock sensors

2. INTRODUCTION

The acceleration environment experienced by the sensors and electronics in an earth-penetrator weapon is extreme, with average accelerations in the 20,000-G range and peak transient accelerations up to

---

* This work was supported by the United States Department of Energy under Contract DE-AC04-94AL85000. Sandia is a multiprogram laboratory operated by Sandia Corporation, a Lockheed Martin Company, for the United States Department of Energy.

^ B.R.D. (correspondence): Email: brdavie@sandia.gov; Telephone: (505) 844-5600
C.C.B. (correspondence): Email: ccbarron@sandia.gov; Telephone: (505) 844-6583
S.M. (correspondence): Email: smonta@sandia.gov; Telephone: (505) 844-6954
J.H.S. (correspondence): Email: smithjh@sandia.gov; Telephone: (505) 844-3098
J.R.M. (MS 1074): Email: jrmurray@sandia.gov; Telephone: (505) 845-9498
T.R.C. (MS 0329): Email: trchris@sandia.gov; Telephone (505) 844-0649
V.I.B. (MS 0555): Email: vibatem@sandia.gov; Telephone (505) 844-0401

several hundred thousand G's. The commercially available accelerometers used in shock testing of earth-penetrator weapons components are both expensive ($1800 each) and prone to failure. Failure analysis of a commercially available sensor was performed at Sandia and will be discussed in the next section. In additiona to failure analysis, a design team was assembled to develop a new micromachined silicon accelerometer which would be capable of surviving and measuring high-G shocks. Such a sensor would presumably be cheaper and more reliable than currently available sensors. Initially, the design team investigated the feasibility of adapting an existing nitride membrane sensor to this environment (described in section 4). Various limitations of this approach were discovered and resulted in the generation of alternate designs. A promising design for a suspended plate mass sensor was developed and will be described in this paper. Future development in this area at Sandia will focus on implementing accelerometers capable of measuring 200 kG accelerations.

3. FAILURE ANALYSIS

Commercially available accelerometers tend to fail due to lack of damping and breaking leads. The only reported silicon-based high-G accelerometers are bulk-micromachined. Preliminary failure analysis of these commercial sensors indicated that failure modes included both undamped high-frequency resonances of the sensor itself and catastrophic failure of the packaging.

We studied a commercially available high-G accelerometer using several failure analysis methods, including optical microscopy, scanning-electron microscopy, electrical testing, acoustic microscopy, and internal impact damage analysis[5]. A total of ten devices were analyzed (five which had not failed and five which had failed during operation). In some lower-G models, chipping and/or complete breakage of the proof mass had occurred.

The dominant failure mode appeared to be directly related to packaging moving mechanical elements. For high-G environments, packaging strength can be significantly enhanced by filling the package with potting material after the chip is installed.

For the commercial high-g accelerometer studied by the design team, two significant failure modes were identified. The package interiors were not completely filled with potting material which resulted in open volumes in the package that allowed particles to move inside the package and damage the moving mechanical elements. Additionally, partial potting may have caused bond wires to fail by acting to amplify shock induced moment loads on the bond wires.

4. ADAPTED MEMBRANE PRESSURE SENSOR

The design team first attempted to design a high-G accelerometer by adapting an existing membrane pressure sensor design to the high-G acceleration environment[1]. A silicon-based pressure sensor, which consists of a circular silicon nitride membrane clamped on all sides and separated from the substrate by an air gap, is shown in Figure 1. Deflections in the membrane are measured by a bridge configuration of piezoresistors patterned on the membrane.

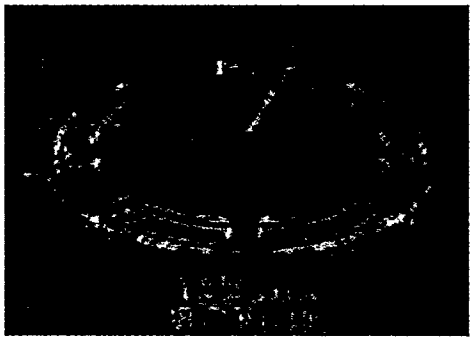

Figure 1: Surface-micromachined pressure sensor manufactured in Sandia's Microelectronics Development Laboratory

The effects of large accelerations normal to the surface of these pressure sensors can be modeled by calculating the equivalent pressure:

$$P = \rho a t, \tag{1}$$

where ρ is the density of the silicon nitride (2330 kg/m^3), a is the acceleration, and t the thickness of the membrane (0.8 μm in the current design). The maximum deflection of the membrane can be estimated according to the following equation:

$$\delta_{max} = [3 P r^4 (1 - \upsilon^2)] / [16 E t^3] = [3 \rho a r^4 (1 - \upsilon^2)] / [16 E t^2] \tag{2}$$

where r is the membrane radius, E is Young's modulus (270 GPa) and υ is Poisson's ratio (0.25) for silicon nitride. For a radius of 125 μm, the predicted deflection is 50 nm at 10,000 G, 1 μm at 200,000 G, and 2.5 μm at 500,000 G, which suggests that this particular sensor will measure up to 200,000 G in either direction normal to the surface.

The diaphragm accelerometer prototypes were packaged using ceramic leadless chip carriers, laser-drilled wire-feed-through holes, Al wedge bonding, and non-conductive thermoplastic die attach.

The suitability of using such a diaphragm design was characterized by packaging existing pressure sensors in a high-G package and testing them in Sandia's shock lab. Shock testing exposed a number of weaknesses in the membrane design. Initial packages survived shock testing up to 50 kG but then failed due to the wire breaking at the heel of the first bond.

It should be noted that these initial samples were not supported by epoxy reinforcement. These packages also had wires extending from the bottom, so that they had to be mounted lid-down on the bar, which introduced some distortion in the detected signal. Newly packaged samples that included bond wires reinforced with epoxy as well as non-reinforced wires were mounted lid-side-up and tested using a Hopkinson bar acceleration testing techniques[2]. Most of these samples failed due to the lid seal breaking.

The adapted membrane sensor design also exhibited high impedance and required an integrated pre-amplifier design that severely restricted their sensitivity. Therefore, a second design was developed which incorporated a suspended plate mass suspended by multiple beam/spring elements. This suspended plate mass design will be further described in the following section.

5. INTEGRATED SUSPENDED MASS ACCELEROMETER DESIGN

A suspended mass high-G accelerometer was designed and fabricated in a variation of Sandia's integrated surface-micromachined polysilicon / electronics manufacturing process. This sensor consists of a parallel-plate capacitor, with one plate stationary with respect to the sensor housing and the second plate suspended by flexible beams that deflect in proportion to the magnitude of the acceleration imposed upon the sensor housing. The sensor was designed to measure accelerations up to 50 kG with a resolution of 50 G. Dominant design tradeoffs include balancing plate deflections sufficient to obtain acceptable signal-to-noise ratios from the capacitive sensors with stiff mass suspension elements necessary to obtain responsive sensor measurements (high bandwidth). Additional design tradeoffs include optimizing response by designing a critically damped system subject to processing constraints. This design takes advantage of Sandia's new integrated surface-micromachining/CMOS manufacturing process to incorporate the capacitive pick-off electronics on-chip. Additionally, multiple sensors were fabricated together on the same chip, so that multiple sensors could be tested with a single shock, and the sensors could be readily used in a redundant, fault-tolerant architecture.

The mechanical elements of the high-G accelerometer were fabricated using two layers of polycrystalline silicon with a separation of 2 μm. The upper layer contains the moving mechanical element of the sensor, and the bottom layer acts as both a structural and electrical ground. The sensor principle of operation is to measure capacitance changes between the two plates with CMOS electronics located adjacent to the mechanical elements (same substrate).

5.1 Accelerometer specifications

Nominal parallel-plate capacitance for the 50 kG sensor is 100 fF at a 2 μm gap. This capacitance level is constrained by the necessity to interface with sensor electronics developed for a previous application. The nominal capacitance requirement and nominal gap spacing translated into a plate overlap area of ≈ 22, 500 μm^2 (≈ 150 μm x 150 μm square area). The desired gap spacing at 50 kG is 1 μm. The resonant frequency of the sensor suspension is constrained to be greater than 100 kHz to accomodate sampling frequencies and the induced vibration caused by the sampling voltage electrostatic attractive force. A target range of 0.4 to 0.6 for damping ratio to obtain adequate response is also desired. This range was dictated more by fabrication considerations, specifically the requirement for sufficient spacing of etch-release holes, and there is very little design flexibility to control damping.

5.2 Mechanical design

The first prototype suspended mass sensor consists of fourteen beam elements (seven on each side) that act as springs to cantilever a 22,600 μm^2 plate mass (top layer of polycrystalline silicon) over a bottom

electrode (bottom layer of polycrystalline silicon). A top view of the sensor and reference capacitor is shown in Figure 2. The sensor consists of two plate masses, one of which serves as a reference capacitor during acceleration measurements. The sensor element on the right is suspended by 14 beams, each 7 μm x 90 μm in size. Each beam acts as a spring allowing the square plate mass in the center of the sensor to move up or down. The reference capacitor, on the left, is a parallel plate capacitor identical in geometry to the sensor parallel plate capacitor with the exception of spring elements. Spring elements in the reference capacitor are designed to be very stiff and at the acceleration levels relevant to sensor operation permit negligible deflection of the plate mass. The reference capacitance and sensor capacitance are compared electronically to measure acceleration.

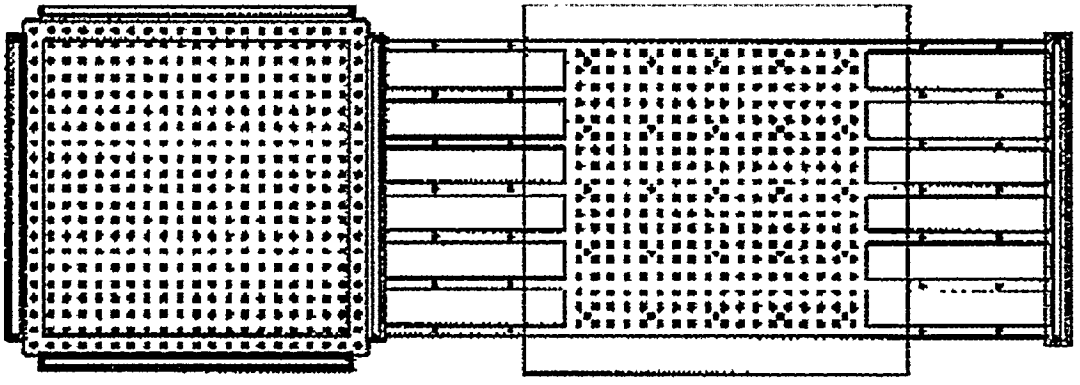

Reference Capacitor **Sensor**

Figure 2: First prototype suspended mass sensor and reference capacitor top view

Each suspended mass is perforated by 324, 2μm x 2μm etch-release holes. The number and spacing of the etch-release holes (necessary for proper fabrication of the sensor element) results in a damping ratio at 50 kG of acceleration of ≈ 0.4. The calculated natural frequency of the sensor is ≈ 127 kHz with a damped natural frequency of ≈ 118 kHz. Cross-axis sensitivity should be minimal and the fracture factor of safety of the device was calculated to be almost three. Results of testing the suspended mass prototype sensor are included in the "Test Results" section of this paper.

Damping was determined by simultaneously applying three different models of squeeze film damping, each of which models some but not all of the applicable characteristics of the suspended mass prototype. (Squeeze-film damping can be defined as the viscous loss of energy due to pumping a viscous fluid out from or into the volume between two moving surfaces.)

The first model[3] is applicable to squeeze-film damping between two parallel disks without perforations that are separated by several μm. In this model, viscous damping occurs due to the movement of fluid around the outside edges of the plates. The damping resistance, R_{film}, is characterized by the following equation:

$$R_{film} = 3\mu S^2/2\pi\delta^3 \qquad (N\cdot s/m) \tag{3}$$

where μ is the fluid viscosity (18×10^{-6} kg/m•s for air at 20 °C), S the plate area overlap, and δ the average plate spacing.

The second model[3] is applicable to squeeze-film damping when one plate is perforated. In this model, viscous damping occurs due to the flow of fluid through the perforations. The damping resistance, R_{perf}, is characterized by the following equation:

$$R_{perf} = 12\mu G(A)S^2/N\pi\delta^3 \qquad (N\cdot s/m) \tag{4}$$

where A is the fraction of open area in the plate, and N is the total number of holes in the perforated plate. The function G(A) is described in equation (5).

$$G(A) = [A/2 - A^2/8 - (\ln A)/4 - 3/8] \tag{5}$$

The third model[3] is applicable to squeeze-film damping at high frequencies (> 10 kHz). This viscous resistance is called radiation resistance and is characterized by the following equation:

$$R_{rad} = \rho c(A\omega/c)^2 \qquad (N\cdot s/m) \tag{6}$$

where ρ and c are the density and speed of sound of the viscous fluid, and ω is the motion frequency.

Each of the three models was applied to the design of the suspended mass accelerometer by modeling each of their respective damping contributions and combining them as parallel elements (as shown in Figure 3).

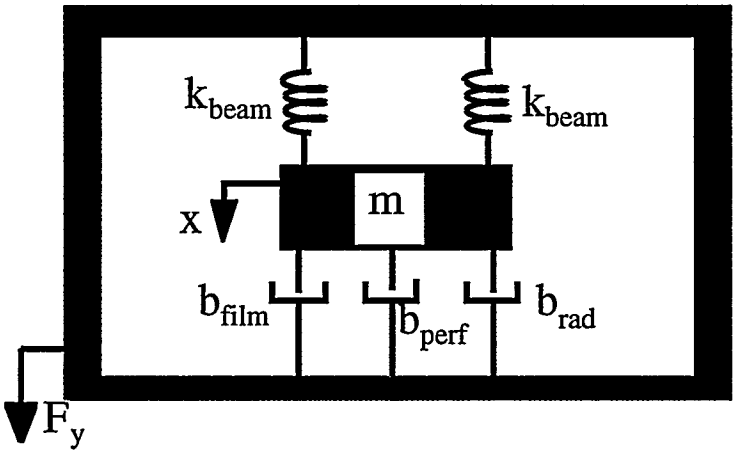

Figure 3: Schematic model for suspended mass accelerometer mechanical elements

5.3. Electrical design

The CMOS circuit for the high-G accelerometer consists of a unity gain buffer followed by a gain stage and output driver. The purpose of the circuit is to measure the change in capacitance of the sensor capacitor relative to the fixed reference capacitor. The sensor capacitor and the reference capacitor are

connected in series and an AC signal (100 kHz, ± 5 V P-P) is applied across the pair. If the two capacitors are not equal, an output signal appears at the common node of the pair. This signal is proportional to the acceleration and is sensed by the CMOS circuit.

Since the sensor capacitors are small, the input capacitance of the circuit is also very small. The first stage consists of an n-channel source follower by an input capacitance of ≈ 40 fF. Noise limits the sensitivity of the circuit, so the circuit was designed to have an input noise of less than 2μV/rt(Hz). The second stage is a combination gain stage and output driver. The gain is ≈ 100 and the output driver is designed to be compatible with the off-chip loads.

Integrating the CMOS electronics on the same substrate as the micromachines enables the microelectronics to measure extremely small capacitance changes (on the order of fractions of atto Farads). This enables the sensor to be operated over a high dynamic range and still measure relatively small changes in acceleration. Additionally, parasitic noise is reduced while bandwidth is increased in the integrated electronics configuration.

6. FABRICATION PROCESS

6.1 Integrated process

Processes for integrating micromechanical devices with their controlling electronics have also been developed at Sandia National Laboratories. Various processing limitations have made it very difficult to fabricate high quality micromachines and high quality CMOS electronics on the same chip substrate. Some of these processing limitations are summarized and discussed by Smith.[4] It is well established that micromechanical structures require long, high-temperature anneals to ensure that the stress in the structural materials of the micromechanical structures has completely relaxed. On the other hand, CMOS technology requires planarity of the substrate to achieve high-resolution in the photolithography process. If the micromechanical processing is performed first, the substrate planarity is sacrificed. If the CMOS is built first, it (and its metallization) must withstand the high-temperature anneals of the micromechanical processing.

A unique micromechanics-first approach has also been developed at Sandia. In this approach, micromechanical devices are fabricated in a trench etched on the surface of the wafer. After these devices are complete, the trench is refilled with oxide, planarized using chemical-mechanical polishing, and sealed with a nitride membrane. The wafer with the embedded micromechanical devices is then processed using conventional CMOS processing. Additional steps are added at the end of the CMOS process in order to expose and release the embedded micromechanical devices. The yield of the most recent lots fabricated using this process has exceeded 98% for integrated combustible gas detection systems.

6.2 Packaging strategy

Sandia's Advanced Packaging Department packaged the sensors to withstand greater than 200,000 G shocks. The approach taken was to encapsulate the accelerometer interconnections without restricting

the movement of the sensor by employing liquid epoxy encapsulation with accurately placed molding dams. Various tests were conducted with different molding compounds to ascertain which molding compounds place the minimum stress on the interconnections. The high frequency moduli was experimentally determined for each molding compound using silicon test chips with built-in stress monitors. Additionally, the merits of different metal geometry's, including standard wire bonding, short beams, and gold bumps were compared and different mounting configurations were tested. Future sensor packaging will only be conducted in areas where the potential for particle introduction is reduced.

Future plans for packaging call for utilizing new stainless steel packages that have been designed and fabricated to meet system requirements. It is anticipated that this will improve assembly performance at increasing shock levels. The custom packages have been received and will be introduced into the packaging of second generation suspended mass prototypes. Additionally, as testing of subsequent devices proceeds up to the 200 kG shock range, the design team will implement appropriate process changes to alleviate any assembly-related failure modes.

7. TESTING

7.1 High-G test capability

The high-G test capabilities available in the SNL Mechanical Shock Lab provided prototype evaluation and characterization of the sensor design. The Shock Lab's Hopkinson-bar testing capability enabled testing of accelerometers to 200,000 G over a frequency bandwidth of DC to 10 kHz; it is currently being upgraded to higher G-levels and a 50 kHz bandwidth. Additional testing capabilities unique to Sandia's Shock Lab include characterization of the cross-axis response of accelerometers, and calculation of sensitivity and frequency response (magnitude, phase, and coherence).
High acceleration testing of both diaphragm prototypes and suspended-mass prototypes was performed using a titanium Hopkinson bar.

7.2 Test results

Preliminary Hopkinson bar test results for the first suspended mass accelerometer prototype demonstrated reasonable correlation between acceleration levels and sensor output at G levels under 15 kG (6 kG, 10 kG, and 14 kG)[8]. At higher G levels (16 kG), sensor output could not be correlated to acceleration level.

The suspended mass accelerometer output signals also appeared to contain carrier signal components, shock signal artifacts, and unidirectional output bias. A filtered sample test trace is included in Figure 4. The design team examined probable causes for the observed reduction in sensor performance. A number of electronic as well as mechanical issues were identified and addressed that likely contributed to the sensors' operation. These issues included residual stress in the suspended mass suspension, resonant overtravel, output bias, underdamped mass motion, output amplifier saturation, excessive design gain, and incomplete comparator signal cancellation.

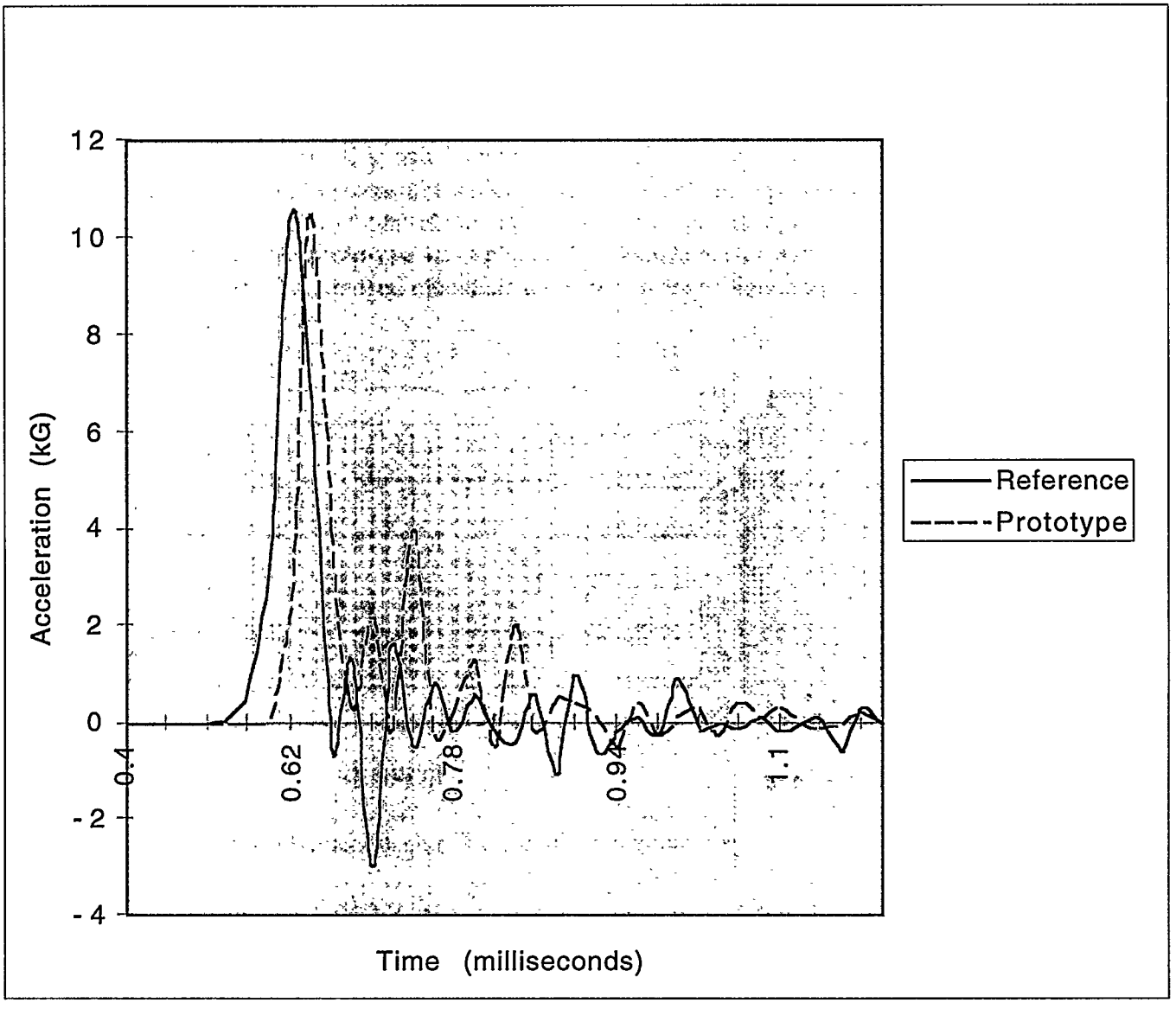

Figure 4: Filtered acceleration vs. time trace for suspended plate accelerometer test at 10 kG

Each likely performance degradation issue was evaluated and incorporated into the second generation prototype design. A discussion of the revised design is included in the next section.

Additional testing will be undertaken to chacterize sensor performance further. Sensor chips will be subjected to a series of acceleration levels to characterize repeatability and correlation, as well as probable electronics saturation and discrimination levels. Additionally, several chips will be tested at excessive accelerations (up to 200 kG) in order to evaluate bonding and packaging performance at severe acceleration levels.

8. REVISED DESIGN

ACKNOWLEDGMENTS

The authors wish to express their sincere appreciation to David Ryerson for program direction, Vesta Bateman for shock testing, Danny Rey for electronics testing, W. Doyle Miller for packaging the sensor, Todd Christenson for leading the failure analysis, and Tom Gugliotta for fabricating the prototype sensors. Without the outstanding assistance of these dedicated professionals, the work described above could not have been accomplished.

REFERENCES

1. W. P. Eaton and J. H. Smith, "Planar Surface-Micromachined Pressure Sensor with a Sub-Surface Embedded Reference Pressure Cavity", *Proceedings of SPIE Micromachined Devices and Components II*, Vol. 2882, October, 1996.

2. T. C. Togami, W.E. Baker, and M.J. Forrestal, "A Split Hopkinson Bar Technique to Evaluate the Performance of Accelerometers", *Journal of Applied Mechanics*, June, 1996.

3. T. B. Gabrielson, "Mechanical-Thermal Noise in Micromachined Acoustic and Vibration Sensors", *IEEE Transactions on Electron Devices*, Vol. 40, No. 5, May, 1993.

4. J. H. Smith, et. al., "Micromachined Sensor and Actuator Research at the Microelectronics Development Laboratory", SPIE, Vol. 2448, 1995.

5. M. A. Lemkin, M. A. Ortiz, N. Wongkomet, B. E. Boser, "A 3-Axis Surface Micromachined SD Accelerometer", submitted to ISSCC, 1997.

DISCLAIMER